

## A significant enhancement in sintering activity of nanocrystalline $\text{Ce}_{0.9}\text{Gd}_{0.1}\text{O}_{1.95}$ powder synthesized by a glycine-nitrate-process

Dasari Hari Prasad<sup>a,b</sup>, Ji-Won Son<sup>a</sup>, Byung-Kook Kim<sup>a</sup>, Hae-Weon Lee<sup>a</sup>, Jong-Ho Lee<sup>a,\*</sup>

<sup>a</sup>Center for Energy Materials Research, Korea Institute of Science and Technology, Seoul 136-791, Republic of Korea

<sup>b</sup>School of Engineering, University of Science and Technology, 52 Eoeun-Dong, Yuseoung-Gu, Daejeon 305-330, Republic of Korea

Using a glycine nitrate process (GNP), nanocrystalline GDC powder has been successfully prepared that can be sintered at 1200 °C to a relative density of 97% which is a significantly lower sintering temperature compared to that of conventional ceria-based electrolytes prepared by traditional solid state techniques. The effect of the glycine content on the particle size, morphology, and sintering behavior has been studied by changing the glycine-to-nitrate (G/N) ratio during the combustion synthesis. A range of techniques including thermal gravimetric analysis (TGA), Fourier transform infrared spectroscopy (FT-IR), X-ray diffraction (XRD), specific surface area determination (BET), particle size analysis (PSA) and scanning electron microscopy (SEM) were employed to characterize the GDC powders prepared. From the dilatometric studies, it is observed that the GDC powders prepared with a G/N ratio 0.55 show superior sintering activity compared to GDC powders prepared with a lower G/N ratio. A sintered GDC sample showed an ionic conductivity of  $2.01 \times 10^{-2}$  S/cm at 600 °C in air.

**Key words:** Oxides, Combustion Synthesis, Nano-crystalline GDC, Electron microscopy, Electrical conductivity.

### Introduction

Solid oxide fuel cells (SOFCs) have attracted more attention since they were shown to be operable at intermediate temperatures (600-800 °C). In this temperature range, it is expected to decrease material degradation and prolong stack lifetime, and reduce cost by utilizing inexpensive metallic interconnects [1, 2]. Increased resistance of the electrolyte caused by the lowered operating temperatures can be addressed either by decreasing the electrolyte thickness or by introducing alternative materials with higher ionic conductivity at lower temperatures. With a high ionic conductivity between 500 and 800 °C, doped ceria has been extensively studied as electrolytes in reduced-temperature SOFCs [3-6]. Gadolinia-doped ceria (GDC,  $\text{Ce}_{0.9}\text{Gd}_{0.1}\text{O}_{1.95}$ ) is considered to be one of the most promising electrolytes for SOFCs to be operated below 700 °C [4]. Furthermore, doped ceria has also been successfully used as part of the anode which can be directly used for hydrocarbon fuels [3].

Various synthesis methods such as homogeneous precipitation [7-12], a sol-gel process [13], combustion using glycine as fuel [14-20], have been used to prepare doped ceria powder. The GDC powders obtained by wet chemical routes require a sintering temperature of 1400-1600 °C to achieve a high relative density [21, 22].  $\text{CeO}_2$ -based

powders have also been synthesized successfully by combustion synthesis using different fuels such as urea [23, 24], oxalyldihydrazide [25], carbonyldihydrazide [26], and citric acid [27]. Using this combustion synthesis [17-19, 27], the sintering temperature of doped ceria is reduced to 1250-1500 °C to achieve a relative density of over 90%. Among the various combustion methods, the glycine-nitrate-process (GNP) where the fuel is glycine and the oxidizer is a nitrate, is found to be the most suitable method for producing fairly fine, homogenous and complex compositional metal oxide powders. In addition, GNP has many other advantages such as a relatively low cost, high energy efficiency, fast heating rates, short contact times and compositional homogeneity [28-31]. Mukasyan *et al.* [32] have defined three combustion modes depending on the glycine to nitrate (G/N) ratio for  $\text{La}_{0.8}\text{Sr}_{0.2}\text{CrO}_3$  where the G/N ratio is a critical factor which determines the powder characteristics; smoldering combustion synthesis (SCS):  $G/N < 0.39$ ,  $T < 600$  °C; volume combustion synthesis (VCS):  $0.39 < G/N < 0.66$ ,  $1150$  °C  $< T < 1350$  °C; self-propagating high-temperature synthesis (SHS):  $0.66 < G/N < 0.88$ ,  $800$  °C  $< T < 1100$  °C. Recently, Mokkelbost *et al.* [20], observed an increase in ignition temperature with increasing G/N ratios upto 0.55 whereas there were no observed changes above 0.55.

The aim of our investigation is to study the synthesis of high quality nano-crystalline GDC fine particles with a narrow size distribution to achieve a lower sintering temperature and high sinterability using GNP. The effect of the glycine content on the crystallite size, particle size, surface area, and sintered density is examined by varying

\*Corresponding author:  
Tel : +82 29585532  
Fax: +82 29585529  
E-mail: jongho@kist.re.kr

the glycine to nitrate (G/N) ratio ( $0.1 \leq G/N \leq 0.55$ ) where a G/N ratio of 0.55 is the stoichiometric ratio. The sintering behavior of these powders was examined along with microstructural observations of the sintered samples. Finally the electrical properties of highly dense pellet specimens were determined. A clear co-relationship between the characteristics of GDC nano particles and the sintering behavior is discussed in terms of the nature of the agglomeration (soft or hard) and the pore size distribution.

## Experimental

### Powder preparation

Nano crystalline GDC powders were prepared by a glycine-nitrate-process. Individual solutions of cerium nitrate hexahydrate ( $Ce(NO_3)_3 \cdot 6H_2O$ , Kanto chemicals) and gadolinium (III) nitrate hexahydrate ( $Gd(NO_3)_3 \cdot 6H_2O$ , Aldrich) were made by dissolving the nitrates in distilled water. The solutions were mixed in appropriate proportions for a nominal composition of GDC and glycine (Junsei Chemicals) was added in the range of a G/N ratio 0.1 to 0.55 as the fuel for combustion. Glycine plays a dual role in this process; first, it prevents the selective precipitation as the water is evaporated and second, it serves as a fuel for the combustion reaction, being oxidized by the nitrate ions. The resulting solution was stirred for 2 h and boiled to evaporate excess water. Combustion was carried out in a fume hood in a large volume beaker on a hot plate. The hot plate was heated up and the solution was allowed to boil until it thickened and become ignited. The beaker was covered with a nickel mesh to contain the ash. The powder obtained was calcined at 600 °C for 2 hours to remove any trace amounts of carbon. Further to reduce the particle size and to achieve a fine particle size distribution the GDC powder prepared with a G/N ratio of 0.55 was ball milled for 12 hours.

In order to examine the sintering behavior, the calcined powders were pelletized and pressed with a pressure of 200 MPa using cold isostatic pressing (CIP). With a heating and cooling rate of  $3 \text{ K} \cdot \text{minute}^{-1}$ , the pellets prepared with ball milled GDC powders and from various G/N ratios were sintered at 1200 °C and 1300 °C for 3 hours.

### Characterization

The phase and crystallinity of the calcined oxide powders were determined by an X-ray diffractometer (PW 3830 X-ray generator, Netherlands). Thermo-gravimetric analysis (TGA) (Netzsch STA 409 PC, Germany) was carried on the as-prepared GDC powders. Infrared spectra of the as-prepared powders were recorded in the  $400\text{--}4000 \text{ cm}^{-1}$  range (IR 300 Spectrometer, Thermo Mattson, U.S.A) by preparing KBr (Merck for spectroscopy) pellets (0.5 wt% sample). The specific surface area of the powders was measured by BET (Quantachrome Corporation Autosorb, U.S.A). The nature of agglomerates of the powders was identified using ultrasonication (Sonosmasher, ULSSO Hi-tech, South Korea) and a particle size analyzer (Microtrac

UPA 150, U.S.A). 2 wt% ploy-vinylpyrrolidone (PVP) was used as a dispersing agent. The density of the sintered pellets was determined by the Archimedes method and expressed as relative to the theoretical density of GDC. EDS/SEM (XL-30 FEG ESEM, Netherlands) was used for the compositional and microstructural analysis such as size, shape and morphology of the powder obtained and its agglomerates. For the sintering behavior and conductivity measurements the prepared pellets were pressed at 200 MPa by using cold isostatic pressing (CIP). The pore size distributions of the green compacts were determined by mercury penetration porosimetry (Micro-meritics, Autopore IV, 9500, Norgross, USA). The shrinkage of the green bodies up to 1500 °C was measured with a dilatometer (Netzsch Dil 402C/3/G, Germany) in air with a heating rate of  $3 \text{ K} \cdot \text{minute}^{-1}$ . The conductivity of the sintered pellet specimens was measured in the temperature range of 400–900 °C in air using a potentiostat/galvanostat IVIUMSTAT, Netherlands) with a four-point probe DC method. Before the measurements, Pt paste was painted onto both sides of the sintered pellets and fired at 1000 °C for 1 hour to act as porous gas electrodes.

## Results and discussion

### Powder characteristics

Thermo-gravimetric data for the as prepared GDC powders with different G/N ratios are shown in Fig. 1. From Fig. 1, two major thermal events are observed at 100–200 °C and at above 300 °C. The first one is due to the loss of adsorbed  $H_2O$  and  $CO_2$  on the surface of the powder and the second one is caused by decomposition of the nitrates present in the powders. As the G/N ratio decreases, the amount of surface adsorbed  $H_2O$  and  $CO_2$  released at 100–200 °C increases during the heat treatment of the samples. Additionally, a larger weight loss due to removal of the nitrate species occurring at above 300 °C is

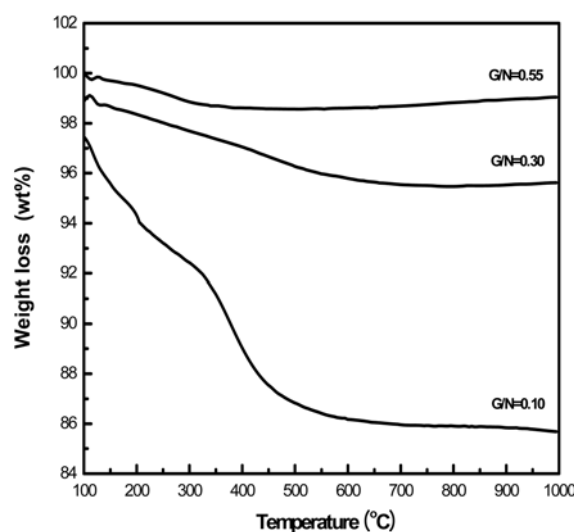
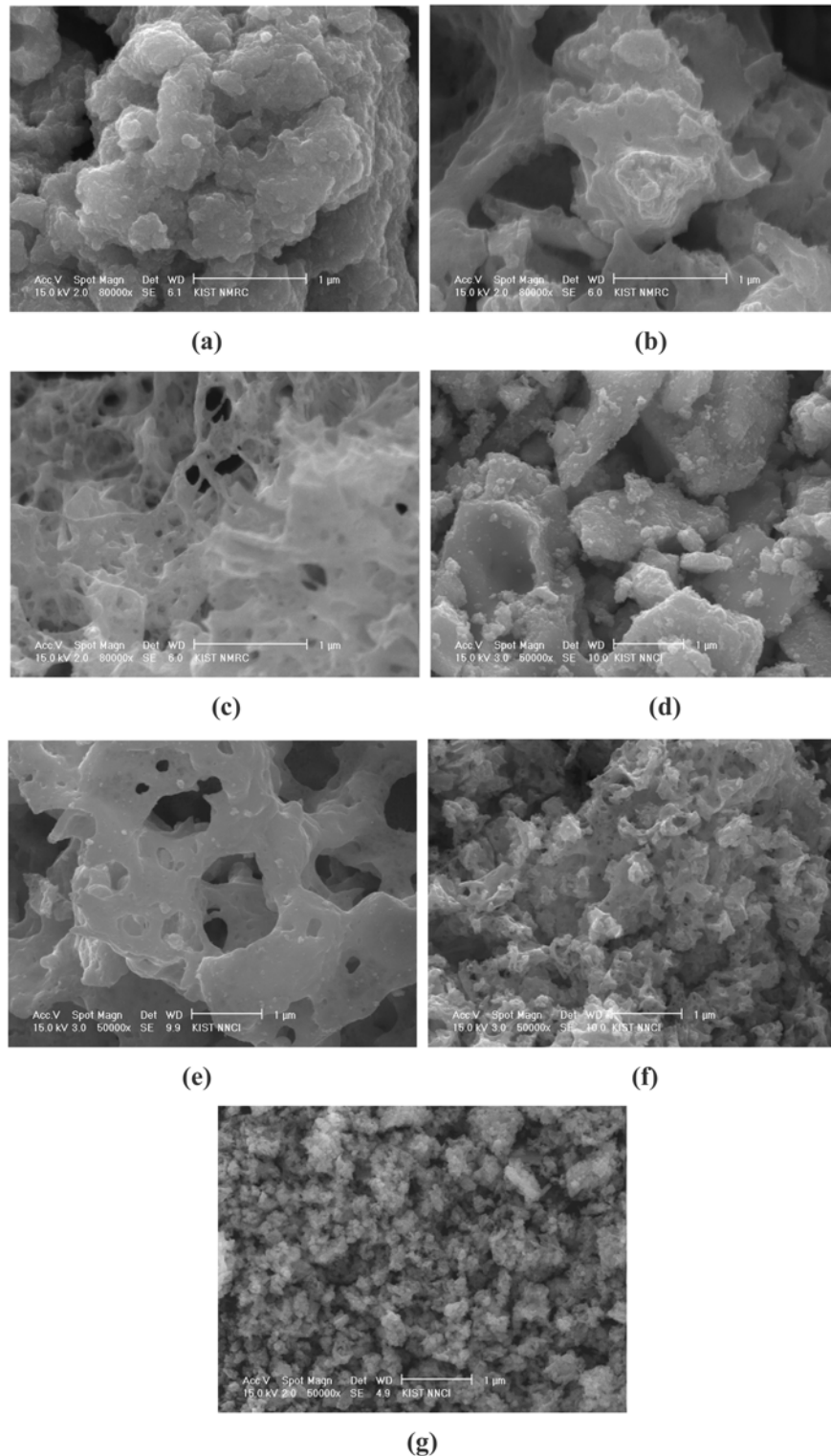


Fig. 1. TG Analysis of the as-prepared GDC powders by the glycine-nitrate process with different G/N ratios.

observed in low G/N ratio samples. Due to incomplete combustion during the reaction, small amount of nitrates may still be present in the powders with G/N ratios of 0.3 and 0.1 and this may be the reason for the weight loss in these samples at above 300 °C as this temperature

correspond to decomposition of the nitrates that are present in the precursors. Similar results were observed by Mokkelbost *et al.* [20] for pure CeO<sub>2</sub> powder prepared by a GNP method.

Fig. 2 shows SEM images of Ce<sub>0.9</sub>Gd<sub>0.1</sub>O<sub>1.95</sub> as-prepared



**Fig. 2.** SEM images of as-prepared GDC powders with G/N ratios (a) 0.1 (b) 0.3 (c) 0.55 and 600 °C calcined GDC powders with G/N ratios (d) 0.1 (e) 0.3 (f) 0.55 and (g) ball milled GDC (G/N = 0.55).

powders with different G/N ratios. It can be observed from Fig. 2 that as the G/N value increases the porous nature of the powder also increases. Fig. 2(g) shows the SEM image of the ball milled GDC powder prepared with a G/N ratio of 0.55, which indicates the size of the agglomerates has been reduced after ball milling. FT-IR Spectra of the as-prepared GDC powders produced with different G/N ratios are shown in the Fig. 3. The main features of the IR spectra are bands in the 1200-1700  $cm^{-1}$  and 3000-3800  $cm^{-1}$  regions. Bicarbonate-like species and mono-dentate carbonate species with O-C-O stretching frequencies of 1620  $cm^{-1}$  and 1430-1460  $cm^{-1}$  are observed [20, 33]. The bands in the region 3000-3700  $cm^{-1}$  can be attributed to O-H stretching of physisorbed  $H_2O$  or from surface Ce-OH groups [20]. At low G/N ratios formation of bidentate carbonate species occurs as a band at  $\sim 1330\text{ cm}^{-1}$  is observed. The strong band at 1383  $cm^{-1}$  might be due to physically adsorbed  $CO_2$  due to the sharpness of the band. From the result that the overall intensity of the bands decreases as the G/N ratio increases, we could recognize that relatively pure GDC powders can be obtained as the G/N ratio is increased, without any contamination by carbonate species and physisorbed  $H_2O$  [20, 34].

XRD patterns of the GDC powders with different G/N ratios calcined at 600 °C for 2 h are shown in Fig. 4.

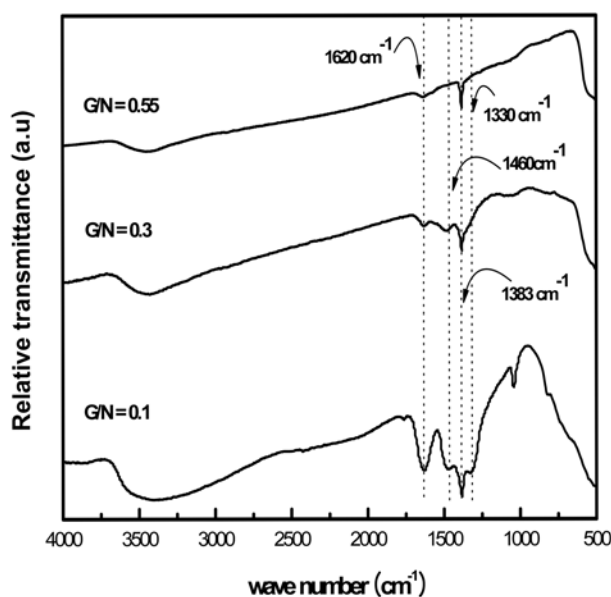


Fig. 3. FT-IR analysis of the as-prepared GDC powders with different G/N ratios

All the powders prepared showed the main reflections of GDC with a typical cubic fluorite structure corresponding to (111), (200), (220), (311), (222) and (400) planes (JSPDS No 75-0161). From Table 1, it can be observed that as the G/N ratio increases the crystallite size also increases slightly and this can be due to increases in the reaction flame temperature. Table 2 shows EDS analyses of GDC samples prepared with different G/N ratios and confirms the composition of the samples.

A particle size analyzer along with ultrasonication to break the agglomerates has been used in order to identify the nature (soft or hard) of agglomerates formed in the calcined powders prepared with different G/N ratios. Table 1 shows the change of average agglomerate size

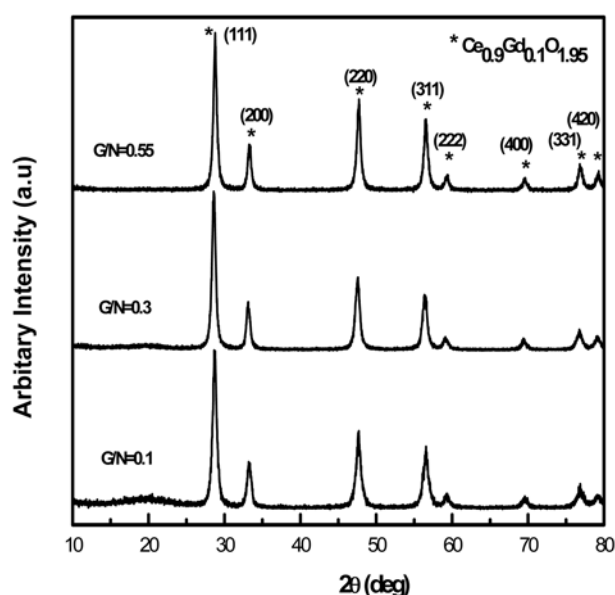


Fig. 4. XRD patterns of GDC powders calcined at 600 °C for 2 h with different G/N ratios.

Table 2. Compositional analysis of the GDC powder calcined at 600 °C for 2 h with different G/N ratios using EDS

GDC powder calcined at 600 °C/2 h	Element	Wt%	mol%
G/N = 0.1	Ce	87.14	87.59
	Gd	13.85	12.40
G/N = 0.3	Ce	89.2	90.27
	Gd	10.78	9.72
G/N = 0.55	Ce	89.22	89.35
	Gd	11.93	10.64

Table 1. Crystallite Size, Particle Size, Agglomerate size and Surface Area of GDC powders calcined at 600 °C /2 h synthesized by the glycine-nitrate-process with different G/N ratios

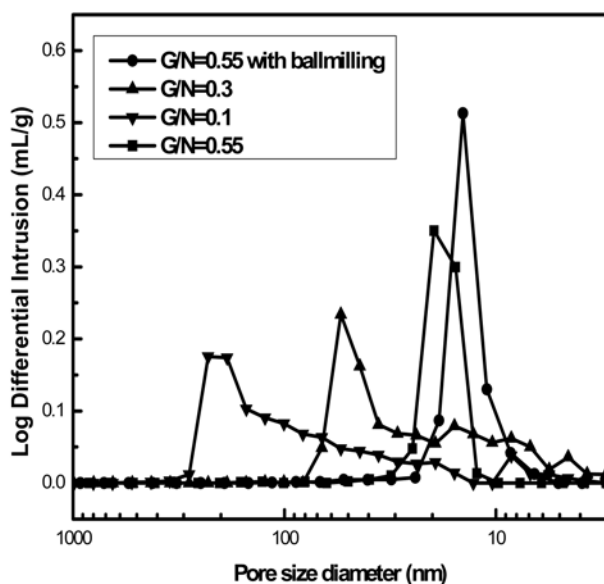
GDC powder calcined at 600 °C/2 h	G/N = 0.1	G/N = 0.3	G/N = 0.55 Without ball milling	G/N = 0.55 With ball milling
Crystallite size (nm)	14	16	17	17
Avg. Agglomerate Particle size (nm) (after ultra-sonication)	2700	2305	578	250
Surface area (m <sup>2</sup> /g)	22	18	38	45

of the powders after ultrasonication. Before ultrasonication the GDC powders with different G/N ratios showed almost the same agglomerated particle size of around  $\sim 3.2 \mu\text{m}$  but after the ultrasonication the agglomerated particle size decreases with an increase of the G/N ratio. This indicates that at a higher G/N ratio, a complete combustion reaction takes place with vigorous evolution of gases which results in the formation of softer agglomerates which can be broken more easily. The ultrasonication time was optimized and fixed to 20 minutes (Figure is not given for brevity). However, excess ultrasonication time causes the rise of the suspension temperature and hence an increase of the average agglomerate particle size, which is thought to be related to the excessive micro-air bubbles generated by the gasification effect and the electric charge from intense friction [35].

### Sintering behavior

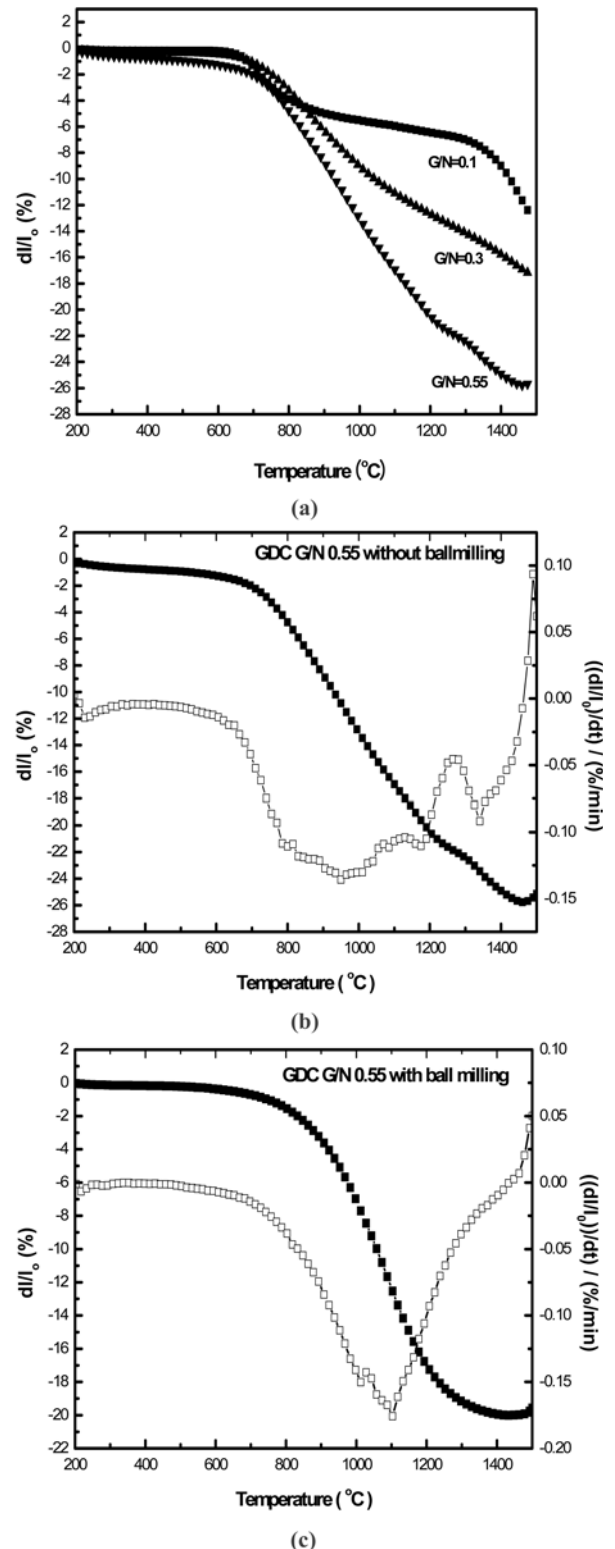
Fig. 5 illustrates the pore size distribution curves for the green compacts prepared by the glycine nitrate process with different G/N ratios. From this figure it can be observed that as the G/N ratio increases from 0.1 to 0.55, the pore size diameter decreases. The samples with lower G/N ratios showed wider pore size distributions especially compared to the ball milled GDC. In the case of the ball milled GDC compact, a very narrow and unimodal pore size distribution with only one maximum centered at 14 nm is observed and these pores can be eliminated at a lower sintering temperature. GDC samples prepared with G/N ratios of 0.1 and 0.3 showed a broader pore size distribution curves centered around 210 nm and 55 nm respectively, as a consequence of both a higher degree of agglomeration and denser agglomerates, these samples can show a lower sinterability.

Fig. 6. shows the dilatometric studies of GDC with



**Fig. 5.** Pore size distribution curves for the GDC green compacts with different G/N ratios.

different G/N ratios. From Fig. 6(a) it can be observed that the liner shrinkage of the GDC samples starts at  $700^\circ\text{C}$  and reached up to 12%, 17% and 26% at  $1500^\circ\text{C}$



**Fig. 6.** Sintering behavior of GDC powders synthesized by the glycine-nitrate-process (a) Linear Shrinkage of GDC with different G/N ratios (b) Linear Shrinkage and Shrinkage rate of GDC (G/N = 0.55) without ball milling (c) Linear Shrinkage and Shrinkage rate of GDC (G/N = 0.55) with ball milling

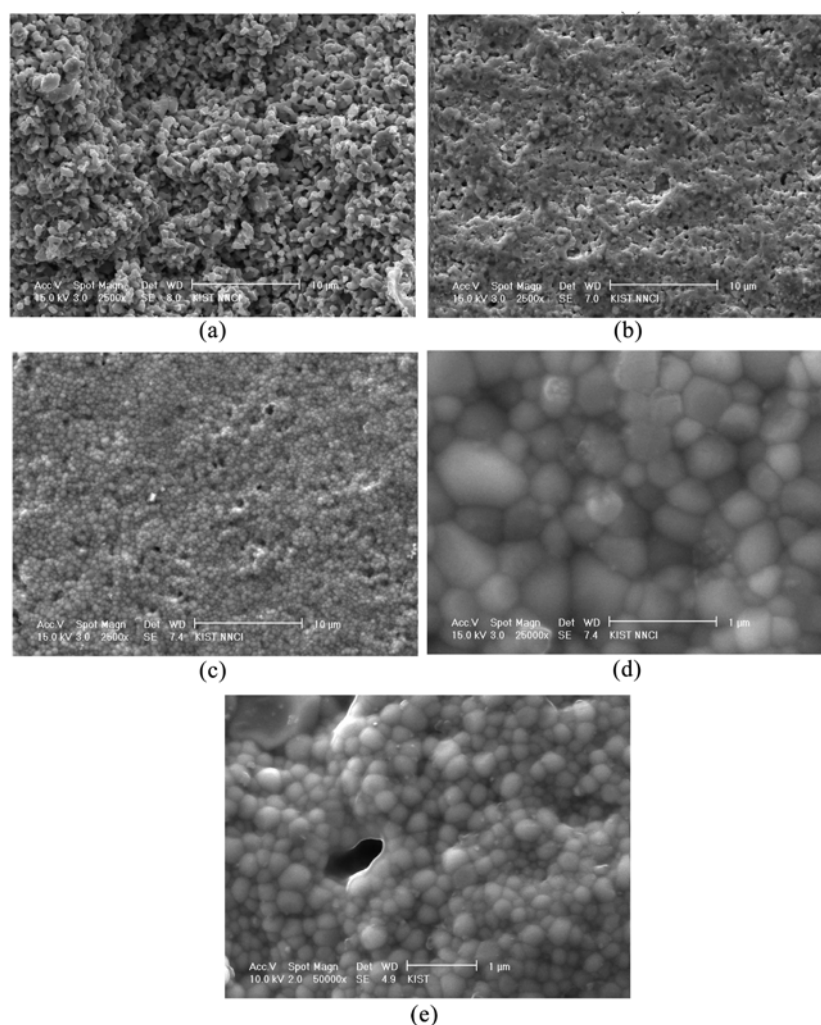
for GDC samples prepared with G/N ratios 0.1, 0.3 and 0.55, respectively. In the case of GDC samples with G/N ratios 0.1 and 0.3, the linear shrinkage and shrinkage rate is very low mainly due to their larger particle sizes, and formation of harder agglomerates (See Fig. 2(d), (e), and Table 1) and wider pore size distribution (See Fig. 5). However, the GDC powder with a G/N ratio of 0.55 can be sintered at a lower sintering temperature, which can be attributed to a relatively smaller particle size and formation of softer agglomerates (see Fig. 2(f) and Table 1).

Fig. 6(b) and (c) show the linear shrinkage and shrinkage rate spectra of before and after the ball milling of GDC samples prepared with G/N ratio of 0.55. As shown in Fig. 6(b), the shrinkage rate spectra of GDC samples without ball milling showed three different shrinkage maxima at 950 °C, 1150 °C, and 1350 °C. The appearance of these shrinkage maxima may be due to different inter-particle pore sizes in the green compact. As shown in Fig. 2(f), the irregular shaped GDC powder prepared with a G/N ratio of 0.55 may have induced a relatively wider pore size distribution in the green compact and showed various peak positions in shrinkage maxima with

respect to the differences in pore size. For example, the larger pores required a higher temperature and longer time for them to be removed whereas smaller ones can be eliminated at a relatively lower temperature. On the other hand, the ball milled GDC sample showed only one shrinkage maximum at a relatively lower temperature of 1100 °C (See Fig. 6(c)) which indicates that the pore size distribution becomes narrower and approaches nearly a mono-size system. Furthermore elimination of hard agglomerates after ball milling could reduce the sintering temperature down to 1200 °C.

### Microstructure and electrical conductivity

Fig. 7(a)-(c) shows SEM micrographs of the GDC samples sintered at 1300 °C for 3 h with G/N ratios of 0.1, 0.3 and 0.55, respectively, prepared from the powders calcined at 600 °C for 2 h. Some small pores still existed in the sintered samples prepared with G/N ratios 0.1 and 0.3 and a very small porosity was observed for the sintered sample prepared with a G/N ratio of 0.55. This demonstrates that a higher sintering activity was achieved for GDC powders prepared with a G/N ratio of 0.55



**Fig. 7.** SEM images of the GDC samples sintered at 1300 °C for 3h prepared with G/N ratios (a) 0.1 (b) 0.3 (c) 0.55. Magnified image of (d) GDC (G/N = 0.55) sample (e) Ball milled GDC (G/N = 0.55).

**Table 3.** Sintered and relative density (%) of GDC samples prepared with different G/N ratios

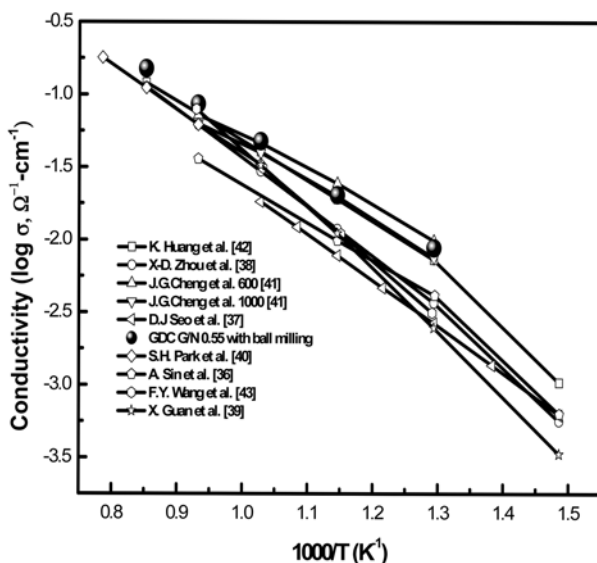
GDC pellets	Theoretical density (g/cm <sup>3</sup> )	Green density (g/cm <sup>3</sup> )	Sintered density (g/cm <sup>3</sup> )	Relative density (%)	Sintering temperature (°C)
G/N = 0.1	7.226	3.17	4.78	66	1300
G/N = 0.3	7.226	3.25	5.85	81	1300
G/N = 0.55	7.226	3.39	6.91	95	1300
G/N = 0.55	7.226	3.68	7.04	97	1200

With Ball milling

compared to the powders prepared with other G/N ratios.

Table 3 shows the green, sintered and relative densities of GDC samples prepared with different G/N ratios. Ball milled GDC showed the highest green density due to the fairly uniform and small particle size as compared to other GDC powders. Even at a relatively lower sintering temperature of 1200 °C, ball milled GDC showed a higher relative density of 97% when compared to other GDC samples sintered at 1300 °C. Fig. 7(d) is a magnified image of Fig. 7(c), which shows that the GDC sample prepared with a G/N ratio of 0.55 is almost fully dense with a grain size of about 0.3-0.5 µm. On the other hand, as shown in Fig. 7(e), the ball milled GDC sample sintered at 1200 °C has a smaller grain size of about 0.1-0.3 µm than the sample without ball-milling.

Fig. 8 presents the electrical conductivity of the ball milled GDC sample prepared with a G/N ratio of 0.55 after ball milling and sintering at 1200 °C. The conductivity in Fig. 8 represents the ionic conductivity because doped ceria is known to behave as a pure ionic conductor in air with negligible electronic conductivity. As shown in Fig. 8, the ionic conductivity increases as the temperature increases with an activation energy of 0.61 eV. Typical ionic conductivity of this sintered GDC sample was about  $2.01 \times 10^{-2} \Omega^{-1} \text{cm}^{-1}$  at 600 °C which matches well with other reported values [4, 36-43].

**Fig. 8.** Temperature dependence of conductivity of various GDC samples in air.

## Conclusions

Nano-crystalline GDC powders with different G/N ratios (0.1, 0.3 and 0.55) were successfully prepared by a glycine-nitrate-process. From a thorough investigation of the effect of the glycine content on the crystallite size, particle size and final density, we found that a G/N ratio of 0.55 was the optimum condition to get high quality GDC powders which have a smaller particle size and fairly soft agglomerates. Formation of softer agglomerates with a smaller particle size in turn could decrease the sintering temperature down to 1200 °C which is a significantly lower sintering temperature compared to that of conventional ceria based electrolytes prepared by traditional solid state techniques. In addition, a fairly high ionic conductivity of  $2.01 \times 10^{-2} \Omega^{-1} \text{cm}^{-1}$  at 600 °C in air could show the potential of this GDC powders for the application as an SOFC electrolyte.

## Acknowledgments

This work was supported by the Institutional Research Program and NRL Program of Korea Institute of Science and Technology.

## References

1. B.C.H. Steele and A. Heinzl, *Nature* 414 (2001) 345-352.
2. S.M. Haile, *Acta Mater.* 51 (2003) 5981-6000.
3. S. Zha, A. Moore, H. Abernathy and M. Liu, *J. Electrochemical Soc.* 151[8] (2004) A1128-A1133.
4. B.C.H. Steele, *Solid State Ionics* 129 (2000) 95-110.
5. M. Mogensen, N.M. Sammes and G.A. Tompett, *Solid State Ionics* 129 (2000) 63-94.
6. M. Sahibzada, B.C.H. Steele, K. Hellgardt, D. Barth, A. Effendi, D. Mantzavinos and I.S. Metcalfe, *Chem. Eng. Sci.* 55 (2000) 3077-3083.
7. J. Van Herle, T. Horita, T. Kawada, N. Sakai, H. Yokakawa and M. Dokiya, *J. Am. Ceram. Soc.* 80 (1997) 933-940.
8. S.W. Zha, Q.X. Fu, Y. Lang, C.R. Xia and G.Y. Meng, *Mater. Lett.* 47 (2001) 351-355.
9. Y. Gu, G. Li, G. Meng and D. Peng, *Mater. Res. Bull.* 35 (2000) 297-304.
10. J.G. Li, T. Ikegami and T. Mori, *Acta Mater.* 52 (2004) 2221-2228.
11. A.I.Y. Tok, L.H. Luo and F.Y.C. Boye, *Mater. Sci. Eng. A* 383 (2004) 229-234.
12. T.J. Kirk and J. Winnick, *J. Electrochem. Soc.* 140 (1993) 3494-3496.

13. W. Huang, P. Shuk and M. Greenblatt, *Solid State Ionics* 100 (1997) 23-27.
14. C.R. Xia, F.L. Chen and M.L. Liu, *Electrochem. Solid-State Lett.* 4 (2001) A52-A54.
15. R.D Purohit, B.P. Sharma, K.T. Pillai and A.K. Tyagi, *Mater. Res. Bull* 36 (2001) 2711-2721.
16. B. Matovic, S. Boskovic, Lj. Zivkovic, M. Vlajic and V. Krstic, *Mater. Sci. Forum* 494 (2005) 175-180.
17. R. Peng, C. Xia, Q. Fu, G. Meng and D. Peng, *Mater. Lett.* 56 (2002) 1043-1047.
18. L. Dan, L. Zhongyang, Y. Chunjiang and C. Kefa, *J. Rare Earths* 25 (2007) 163-167.
19. C. Xia and M. Liu, *Solid State Ionics* 152 (2002) 423-430.
20. T. Mokkelbost, I. Kaus, T. Grande and M. Einarsrud, *Chem. Mater.* 16 (2004) 5489-549
21. T. Kudo and H. Obayahi, *J Electrochem Soc.* 122 (1975) 142-147.
22. J. Van Herle, T. Horita, T. Kawada, N. Sakai, H. Yokokana and M. Dokiya, *Solid State Ionics* 86 (1996) 1255-1258.
23. E. Chinarro, J.R. Jurado and M.T. Colomer, *J. Euro. Ceram. Soc.* 27 (2007) 3619-3623.
24. C.C. Hwang, T.-H. Huang, J.-S. Tsai, C.-S. Lin and C.-H. Peng, *Mater. Sci. Engg. B* 132 (2006) 229-238
25. S.T. Aruna and K. C.Patil, *Nanostruct. Mater.* 10 (1998) 955-964.
26. S.T. Aruna, S. Ghosh and K.C. Patil, *Int. J. Inorg.Mater* 3 (2001) 387-392.
27. T. Mahata, G. Das, R.K. Mishra, B.P. Sharma, *J alloys and compounds* 391(2005) 129-135
28. L.A. Chick, L.R. Pederson, G.D. Maupin, J.L. Bates, L.E. Thomas and G.J. Exarhos, *Mater. Lett.* 10 (1990) 6-12.
29. J. Kingsley and L.R. Rederson, *Mater. Lett.* 18 (1993), 89-96.
30. D. Hari Prasad, H.-Y. Jung, H.-G. Jung, B.-K. Kim, H.-W. Lee and J.-H. Lee, *Mater. Lett.* 4 (2008) 587-590.
31. L.R. Pederson, G.D. Maupin, W.J. Weber, D.J. McReady and R.W. Stephens, *Mater. Lett.* 10 (1991) 437-443.
32. A.S. Mukasyan, C. Costello, K.P. Sherlock, D. Lafarga and A.Verma, *Sep. Pur. Tech.* 25 (2001) 117-126.
33. V. Bolis, G. Magnacca, G. Carrato and C. Morterra, *Thermochim acta* 379 (2001) 147-161.
34. A. Yee, S.J. Morrison and J. Idriss, *J.Catal* 186 (1999) 279-295.
35. S.-Y. Yao and Z.-H. Xie, *J. Mater. Proc. Tech* 186 (2007) 54-59.
36. A. Sin, Y. Dubitsky, A. Zaopo, A.S. Arico, L. Gullo, D.L. Rosa, S. Siracusano, V. Antonucci, C. Oliva and O. Ballabio, *Solid State Ionics* 175 (2004) 361-366.
37. D.J. Seo, K.O. Ryu, S.B. Park, K.Y. Kim and R.H. Song, *Mater. Res. Bull.* 41 (2006) 359-366.
38. X.-D. Zhou, W. Huebner. I. Kosacki and H.U. Anderson, *J. Am.Ceram. Soc.* 85[7] (2002) 1757-1762.
39. X. Guan, H. Xhou, Z. Liu, Y. Wang and J. Zhang, *Mater. Res. Bull.* 43 (2008) 1046-1054.
40. S.H. Park and Han-Il Yoo, *Solid State Ionics* 176 (2005) 1485-1490.
41. J.G. Cheng, S.W. Zha, J. Huang, X.Q. Liu and G.Y. Meng, *Mater. Chem. Phys* 78 (2003) 791-795.
42. K. Huang, M. Feng and J.B. Goodenough, *J.Am. Ceram. Soc.*, 81 (1998) 357-362.
43. F.Y. Wang, S. Chen, Q. Wang, S. Yu and S. Cheng, *Catal. Today* 97 (2004) 189-194.